IMPACT OF CASTING CONDITIONS ON THE DENDRITIC SOLIDIFICATION IN SINGLE ROLLER QUENCHING METHODS (SIMULATION)

László Gránásy[†] and Andreas Ludwig[‡]

[†]Central Research Institute for Physics, Hungarian Academy of Sciences,
H-1525 Budapest, POB 49, Hungary

[‡]Max-Planck-Institut für Eisenforschung GmbH.,
Max-Planck-Str. 1, D-4000 Düsseldorf, Postfach 140 260, FRG

Abstract

The dendritic solidification under conditions characteristic to the single roller rapid quenching technique has been investigated. The impact of casting conditions (temperature of nucleation, heat transfer coefficient, initial melt- and roller temperature, flow rate and material of the roller) on the growth morphology of crystalline strips has been studied by numerical simulations based on principles described elsewhere (two-dimensional steady state thermal transport, surface induced nucleation, dendritic growth, a simplified treatment of the mushy-zone, L.Gránásy and A.Ludwig, Mater. Sci. Forum, 77 (1991) 211-218). A simple model based on Newtonian cooling has been proposed to describe the effect of casting conditions on surface induced heterogeneous nucleation and on the grain size at the contact surface. The present analysis may contribute to a better understanding of the rapid quenching processing.

Introduction

Microstructure is one of the key factors influencing the physical properties of crystalline alloys. The microstructure of policrystalline alloys may be characterized by two typical lengths: (i) The size of regions of the same crystal orientation (grain size) and (ii) the wave length of fluctuations of chemical composition within a grain. The former is determined by the nucleation and growth rates, while the other is related to the morphology of the advancing crystallization front. Both features may be influenced by the undercooling prevailing during solidification.

Owing to the high cooling rates characteristic to the rapid quenching techniques (melt-spinning, splat cooling, laser glazing, etc.) these methods are especially suitable to achieve high undercoolings during solidification resulting in solids of unusual characteristics. These techniques have successfully been applied for the preparation of different non-equilibrium alloys (metallic glasses, quasi-crystals and microcrystalline materials (1)).

It seems that rapid quenching is one of the most potent means of reducing the grain size (2), while various growth morphologies (cellular, dendritic, banded, helical, etc. (3,4)) and reduction of partitioning can be obtained at high growth rates originating from deep undercooling.

In the past decade a spectacular advance in the understanding of rapid solidification phenomena has been witnessed (3,4). Numerical simulations utilizing the knowledge accumulated on rapid solidification may have an important role in tailoring the microstructure for different applications.

In the present work we study a case quite common in rapid quenching of low and medium freezing range alloys (5-10): The crystallization starts at the melt-roller interface by surface induced nucleation, followed by the formation of a chill zone showing partitionless features or fine scale composition modulations. This structure then gradually changes to a cellular or fully developed solutal dendritic morphology. We are going to develop a model which can reflect this complex behavior. On the basis of the stability analysis by Ludwig (11) we propose a numerical model which includes the formation of oscillating microstructure predicted in previous works (12, 13). Then we report on numerical simulations aimed at finding the connection between microstructure (partitionless growth, banded structure, dendritic growth) and casting conditions. Finally we present a simple model relating grain size to the main technological variables.

Numerical model for cross-sectional changes of morphology

Thermal transport

The heat transport is described by the relevant equation of the boundary layer theory. With the simplified convection term proposed for melt-spinning in (14) the steady state equation is fully analogous to the one-dimensional time-dependent equation. The heat release during solidification is taken into account by a source term:

$$V_o \frac{\partial T}{\partial x} = \alpha \frac{\partial^2 T}{\partial y^2} + V_o \frac{\partial f_s}{\partial x} \cdot \frac{\Delta H_f}{\rho c_p} \qquad (1)$$

where T is the temperature, V_o is the surface velocity of the roller, α is the thermal diffusivity, ρ is the density, c_p is the specific heat, ΔH_f is the heat of fusion, x and y are spatial coordinates parallel and normal to the roller surface, respectively, while f_s is the crystalline fraction, calculated as to be described below. This equation is solved by the explicit finite difference method on a rectangular grid fitted to the experimental geometry. A similar equation, without source term is applied for the thermal transport in the roller. The heat transfer at the melt-roller interface is described by a heat transfer coefficient, h, while the heat radiation on free surfaces is neglected.

Solidification

Nucleation: A surface induced heterogeneous nucleation is assumed at the melt-roller interface. The undercooling necessary for the nucleation is treated as an external parameter.

Crystal growth: One of the most characteristic features of rapid solidification processing is the presence of large cross-sectional thermal gradients in the specimen during solidification (typically 10^7 - 10^8 K/m in case of melt spinning). An analysis by Ludwig (11) indicates that at such temperature gradients the absolute stability limit (V_a, the velocity above which the planar interface is stable) may be lowered to the range of solute limit of absolute stability (V^s_{abs}, typically few times 0.1 m/s). In keeping with this finding, we assume a planar growth morphology for pure metals during the whole solidification process. In case of alloys the planar morphology is restricted to $v > V^s_{abs}$, while a fully developed dendritic morphology is assumed below V^s_{abs}. The advance of the dendrite tips is described by the theory of Kurz, Giovanola and Trivedi (15), while atomic attachment kinetics and solute trapping is taken into account (through a non-equilibrium partition coefficient (16) and liquidus slope (17)). This treatment is strictly valid for the steady state growth of a single dendrite, Zimmermann et al. have shown, however, that it may be applied under rapid quenching conditions as well (18).

The region between the dendrite tips and the front of complete solidification (mushy-zone) is treated as follows. Here - except for the near-tip region - the diffusion field of the dendrites overlap. Because of the complexity of the problem no exact description is available. Following the treatment by Clyne we assume that there exists an $f_s = f_s(T)$ function which describes the variation of the solid fraction with the temperature between the dendrite tip and root (19). Strictly, such a relation exists for steady state and a constant temperature gradient in the mushy-zone. The exact treatment, however, would require the solution of the thermal and solute transport equations for every particular dendrite in the diffusion field of its neighbors which makes the problem much too complicated.

An approximate $f_s = f_s(C_s^*)$ relation has been proposed by Giovanola and Kurz (20), where C_s^* is the composition of the solid:

$$f_s = a_1 \cdot C_s^{*2} + a_2 \cdot C_s^* + a_3 \qquad (0 \le f_s \le f_x), \tag{2a}$$

$$f_s = 1 + (f_x - 1) \cdot \left[\frac{C_s^*}{C_x}\right]^{1/(k-1)} \qquad (f_x \le f_s \le 1), \tag{2b}$$

where f_x, C_x, a_1, a_2 and a_3 are parameters determined from the limiting

values and the mass balance, while k is the partition coefficient. Using the non-equilibrium solidus line obtained with the growth rate dependent partition coefficient this relation can be transformed to an $f_s = f_s(T)$ function. In the present work we adopt this construction. It can be shown that the treatment by Giovanola and Kurz may be applied for growth rates less than $0.05 \cdot V_a$. Thus for $0.05 \cdot V_a < V < V_a$ we apply a different f_s-T relation:

$$f_s = a_1 \cdot C_s^{*2} + a_2 \cdot C_s^{*} + a_3, \qquad (3)$$

where the parameters a_1, a_2 and a_3 are determined from (i) the mass balance and conditions (ii) for $f_s = 0$ $C_s^* = C_{st}^*$ and (iii) at $f_s = 1$ $C_s^* = C_1$. Here C_{st}^* is the concentration of the solid at the dendrite tip, while C_1 is obtained by a linear interpolation between $C_{xe} = C_x|_{v = 0.05V_a}$ from the Giovanola-Kurz treatment (20) and the initial composition of the melt, C_o as a function of growth velocity. This construction ensures a physically reasonable smooth transition from the mushy-zone to a planar interface.

Range of applicability

The analogy between the one-dimensional, time-dependent problem and the two-dimensional steady-state problem is generally considered valid for growth velocities smaller than the roller velocity (21), restricting thus the applicability of the model to small undercoolings. In our opinion the application of the model can be justified for large undercoolings as well: The transformation is clearly valid for short time intervals after nucleation during which back growth of the crystal is negligible in comparison to the dimensions of the problem. If the process is not perturbed, a steady state temperature distribution is established after a transient period in which the leading edge of growth front moves upstream with the velocity of the roller (i.e. stays at a fixed position in the laboratory system). It must be taken into account however, that the heat released by a front perpendicular to the roller and moving with the roller velocity can not be transported away by the typical heat transfer coefficient values. Because of the limitation by heat transport the growth velocity should be about $v = h \cdot (T - T_o)/\Delta H_f$ (at most 1 m/s) for the major part of the growth front. Only a very thin layer may move with the roller velocity. However, it can easily be stopped by the hot regions formed above gas bubbles entrapped between the melt and the roller - at least one on every 100 μm (22) - and the build-up of the steady state has to start again with a new nucleation event. This continuously restarted transient seems to be the typical behavior of the system in which case the analogy is justly applied.

Model for determination of grain size

For sake of simplicity we assume Newtonian cooling conditions which may be an acceptable approximation for the lower limit of the experimental heat transfer coefficient. Under such conditions the cooling of the ribbon is described by the equation

$$\rho \cdot c_p \cdot \delta \cdot \frac{dT}{dt} = - h \cdot (T - T_o) + \frac{dV_x}{dt} \cdot \Delta H_f \qquad (4)$$

where t is time, δ is the ribbon thickness, while V_x is the average thickness of the crystalline layer, determined by the differential equation:

$$\frac{dV_x}{dt} = v \cdot x_s + (1 - x_s) \cdot g \cdot I \cdot r_o^3 + \frac{dx_s}{dt} \cdot \bar{\delta}_s \qquad (5)$$

Here v is the growth velocity, x_s is the fraction of contact surface covered by crystals, g is a geometrical factor depending on the shape of the crystals, I is the nucleation rate, r_o is the size of the critical nucleus, while $\bar{\delta}_s = V_x/x_s$ is the average height of the crystals. The three terms on RHS of eqn. (5) are from the growth normal to the contact surface, from nucleation on the non-crystalline surface and from lateral growth, respectively. Applying the Johnson-Mehl-Avrami (23) approximation the crystalline surface fraction can be expressed by the overlapping crystalline fraction x_s^* as

$$x_s = 1 - \exp(-x_s^*) \qquad (6)$$

where

$$x_s^* = g \cdot \int_0^t I(\vartheta) \cdot \left\{ r_o(\vartheta) + \int_\vartheta^t v(\tau) \cdot d\tau \right\}^2 \cdot d\vartheta. \qquad (7)$$

while ϑ and τ are integration variables of time dimension. For sake of simplicity we assume cylindrical crystals ($g = \pi$) and diffusion controlled nucleation and growth (valid in case of ordered solid solutions and intermetallic compounds). The nucleation rate is taken from the classical nucleation theory:

$$I = \frac{N_s \cdot D}{a_o^2} \cdot \exp\left\{ - \frac{16 \cdot \pi \cdot \gamma^3 f(\theta)}{3 \cdot \Delta g^2 \cdot k_B \cdot T} \right\} \qquad (8)$$

where $N_s = (N_o/v_m)^{2/3}$ is the number density of atoms on surface, N_o is the Avogadro number, v_m is the molar volume, a_o is the diameter of the diffusing specimen, D is the diffusion coefficient, γ is the solid-liquid interfacial free energy, Δg is the volumetric Gibbs free energy difference between the bulk liquid and crystal, while $f(\theta) = (2+\cos(\theta)) \cdot (1-\cos(\theta))^2/4$ gives account for the decrease of free energy of formation of the critical nucleus in case of heterogeneous nucleation, θ is the contact angle between the roller surface and the solid-liquid interface. The growth rate has been described by the equation:

$$v = \frac{D}{a_o} \cdot \left\{ 1 - \exp\left(- \frac{\Delta G}{RT} \right) \right\}, \qquad (9)$$

where ΔG is the molar Gibbs free energy difference between the liquid and the solid and R is the universal gas constant.

Eqns. (5)-(6) have been solved by the finite difference method, while integral (8) have been evaluated numerically using the actual cluster size distribution and the nucleation rate data stored in every time step.

The average grain size was determined from the density of nuclei N_q obtained by integrating $I \cdot (1-x_s)$ until complete solidification of the surface was reached: $d = 2(\pi \cdot N_q)^{-1/2}$.

Physical properties

Data for elements Al, Cu, Fe and Ni were taken from (21) and (24). The relation between casting conditions and growth morphology has been investigated on $Fe_{90.5}Si_{9.5}$. In this case we calculated with the relevant properties of Fe, while the equilibrium distribution coefficient and liquidus slope were read from the phase diagram ($k = 0.75$, $m = -10.6$ K/at.%). Conditions typical for the melt-spinning of 120 μm thick ribbons were used as a reference: Surface velocity = 10 m/s; casting temperature = 1833 K; steel roller of temperature = 700 K; heat transfer coefficient = 0.7 $MWm^{-2}K^{-1}$. The undercooling at nucleation was taken as 300 K. The calculations for grain size were performed for Al_2Cu using the relevant data of Al, except for liquidus temperature and solid-liquid interfacial free energy, which were taken from (25) and (26). The reference conditions have been chosen as follows: Casting temperature 970 K; roller temperature 300 K; heat transfer coefficient = 0.7 $MWm^{-2}K^{-1}$. The Gibbs free energy difference has been calculated by the linear approximation of Turnbull (27).

Results and discussion

Effect of casting conditions on growth morphology

First we investigated the solidification of pure metals Al, Cu, Fe and Ni. In accordance with former calculations with a planar growth morphology (21,28-33) we found that the nucleation is followed by a recalescence phase (see Fig. 1a-b) during which the crystal grows into an undercooled liquid (equiaxial growth) with a growth velocity controlled by atomic attachment kinetics. After this stage directional growth conditions are established and the crystallization becomes thermal transport controlled. In agreement with previous results (21,32-34) changes of the casting conditions which increase the cooling rate (e.g. increasing heat transfer coefficient, decreasing melt and roller temperatures, etc.) tend to reduce the domain of the recalescence effect.

Solute trapping and morphological instability make the solidification in the directional growth phase more complex (34). The growth rate calculated for $Fe_{90.5}Si_{9.5}$ as a function of interface undercooling is presented in Figure 2. Due to the solute trapping effect the curve has a characteristic S-type shape related to the formation of oscillating microstructure by Jönsson (12,13): After nucleation (point N) the system heats up to point A due to the released heat of fusion. Upon further heating, however, growth is possible with only a low velocity, thus the system drops to point B. As a result of the reduced heat release originating from the low growth rate at B the interface temperature decreases. After cooling below point C growth is again possible at only a large interface velocity (point D). This cycle is repeated until the variation of thermal conditions with increasing distance from the roller surface hinders cooling back to point C.

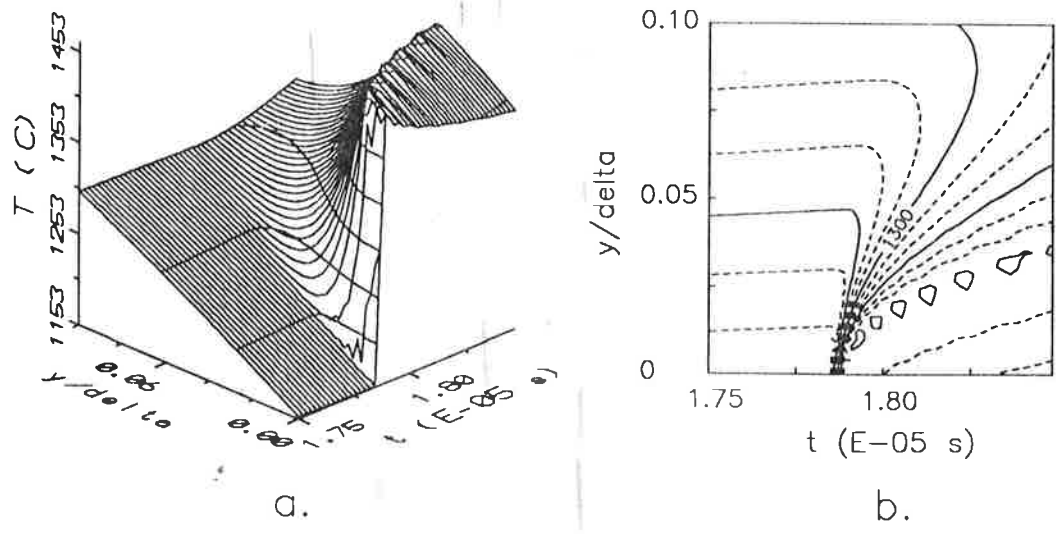

Figure 1 - Recalescence after nucleation calculated for pure Ni. (Thickness = 50 μm; h = 1 $MWm^{-2}K^{-1}$; overheating = 100 K; roller temperature = 300 K; undercooling at nucleation = 300 K; no. of divisions in cross-section = 250.)
a) Distance of contour lines: 50 °C,
b) Distance of contour lines: 25 °C.

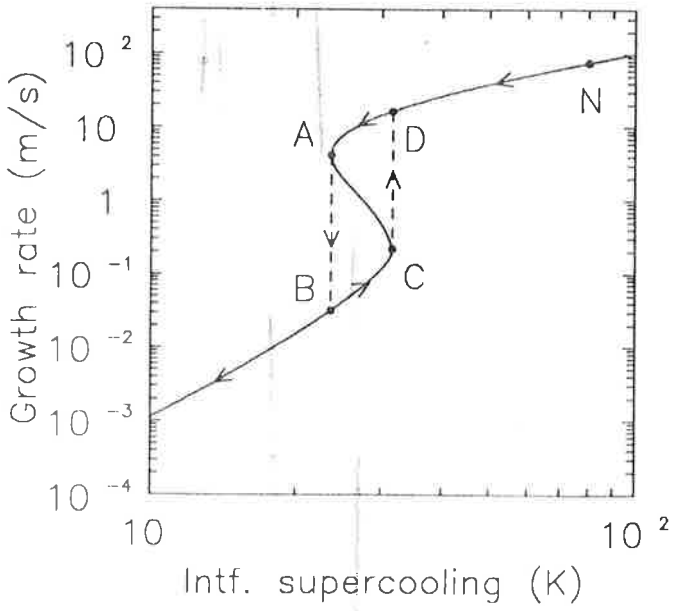

Figure 2 - Growth velocity vs. interface temperature calculated for $Fe_{90.5}Si_{9.5}$. (Notations: N - nucleation; A-D: cycle resulting in oscillating microstructure.)

According to our computations three regions can be distinguished in the cross-section of the ribbons (see Figures 3-10): (i) A partitionless layer near to the contact surface formed by planar growth morphology; (ii) an oscillating region composed of thin partitionless and dendritic layers; and (iii) a dendritic region extending up to the free surface of the ribbon. The characteristic length of the oscillations in region (ii) is about 100 nm in accordance with the data by Jönsson (12,13). Although our numerical resolution should certainly be improved to study the details of the oscillating region, the width of region (ii) is stable against the change of time and spatial steps.

In order to study the relation between casting conditions and the microstructure we have varied the undercooling at nucleation (200 and 300 K), the heat transfer coefficient (0.35 - 1.4 $MWm^{-2}K^{-1}$), the initial melt temperature (100-300 K overheating), the roller temperature (300-700 K), the ribbon thickness (30-120 μm) and the material of roller (Cu, steel and stainless steel). Parameters other than the one investigated were kept at their reference value given in the previous section.

The effect of casting conditions on the three-layered microstructure is shown in Figures 3 - 10. In order to visualize the changes of the solidification process we present the spatial distribution of the solidified fraction (a), the cross-sectional temperature distribution at different positions X of the dendrite tips (b) and the growth rate as a function of interface position (c). To characterize microsegregation in the dendritic zone the solute concentration of the dendrite tips C_{tip} and the composition of the finally solidified melt C_{root} are also given as a function of distance from the roller surface (d).

The most spectacular effect is the variation of the thickness of the partitionless layer (δ_p). δ_p increases with the casting and roller temperatures and decreases with increasing heat transfer coefficient or nucleation temperature. Casting temperature seems to be a suitable technological parameter to control δ_p. Other features, e.g. the thickness of the mushy-zone and banded structure or composition in the dendritic zone are much less sensitive. Figures 9-10 emphasize the importance of the roller material. In case of a copper roller the solidification length and the thickness of the mushy-zone are considerably smaller than for casting on stainless steel. This difference is reflected to some extent even in the microsegregations.

Another important technological parameter is the volumetric rate of flow. Its variation is modeled by changing the ribbon thickness. Our computations show that - as a consequence of the fact that solidification takes place under a melt pool of typical height comparable to the thickness of the thermal boundary layer - the variation of the ribbon thickness does not influence appreciably the solidification: A proportional section of the process for infinite thickness is realized. In other words, the microstructure of a 30 μm thick ribbon is practically identical to that in the lowest 30 μm part of a 120 μm thick ribbon. Thus below a critical ribbon thickness - which depends on the other casting conditions - microsegregation free ribbons can be produced.

Finally, we call attention to the fact that in this analysis the casting parameters are changed independently thus such effects as the variation of the heat transfer coefficient with casting temperature, roller velocity and material of the roller (35) or the variation of nucleation temperature with quenching rate are not taken into account. An investigation of these cross-effects is under way.

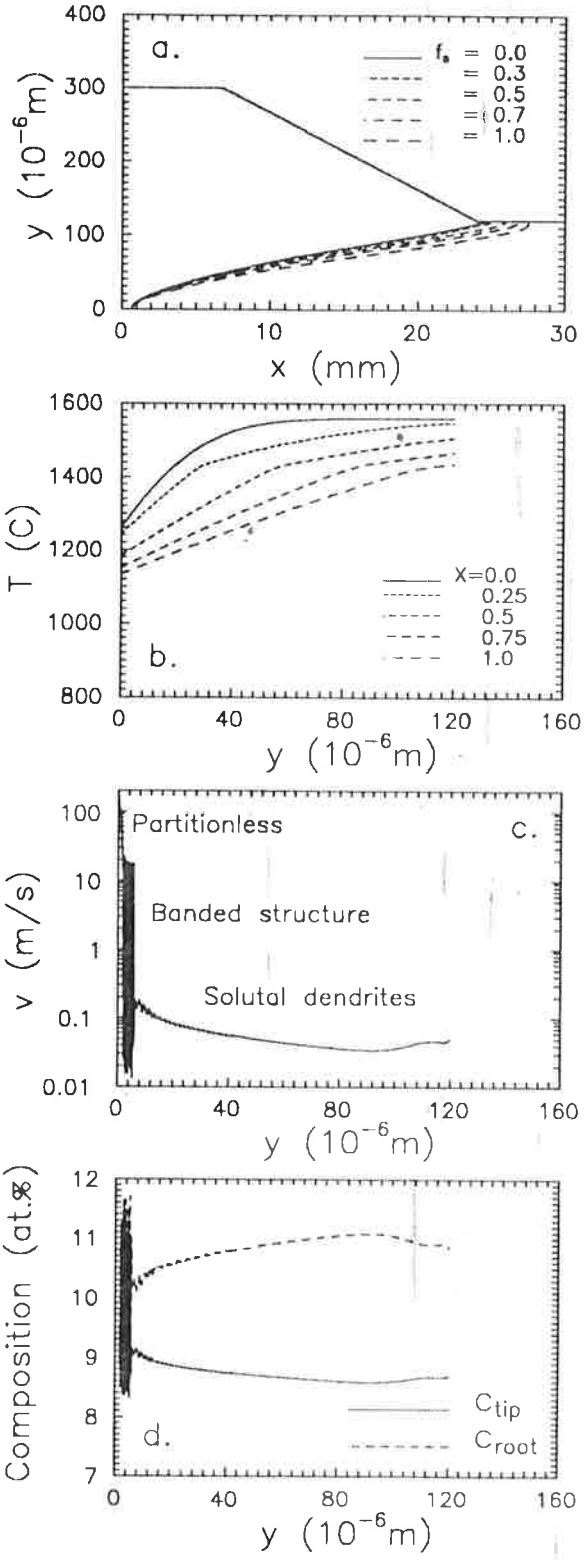

Figure 3

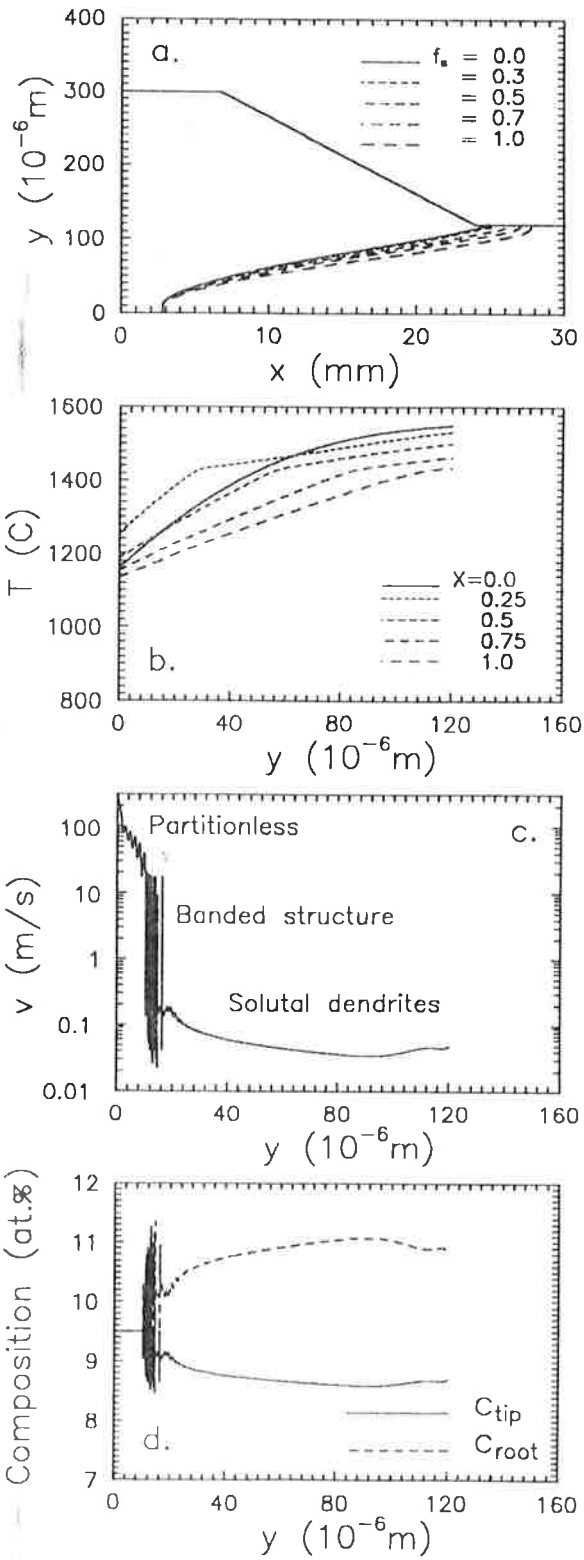

Figure 4

The effect of nucleation temperature on the microstructure:
Undercooling at nucleation: Figure 3 - 200 K,
Figure 4 - 300 K.

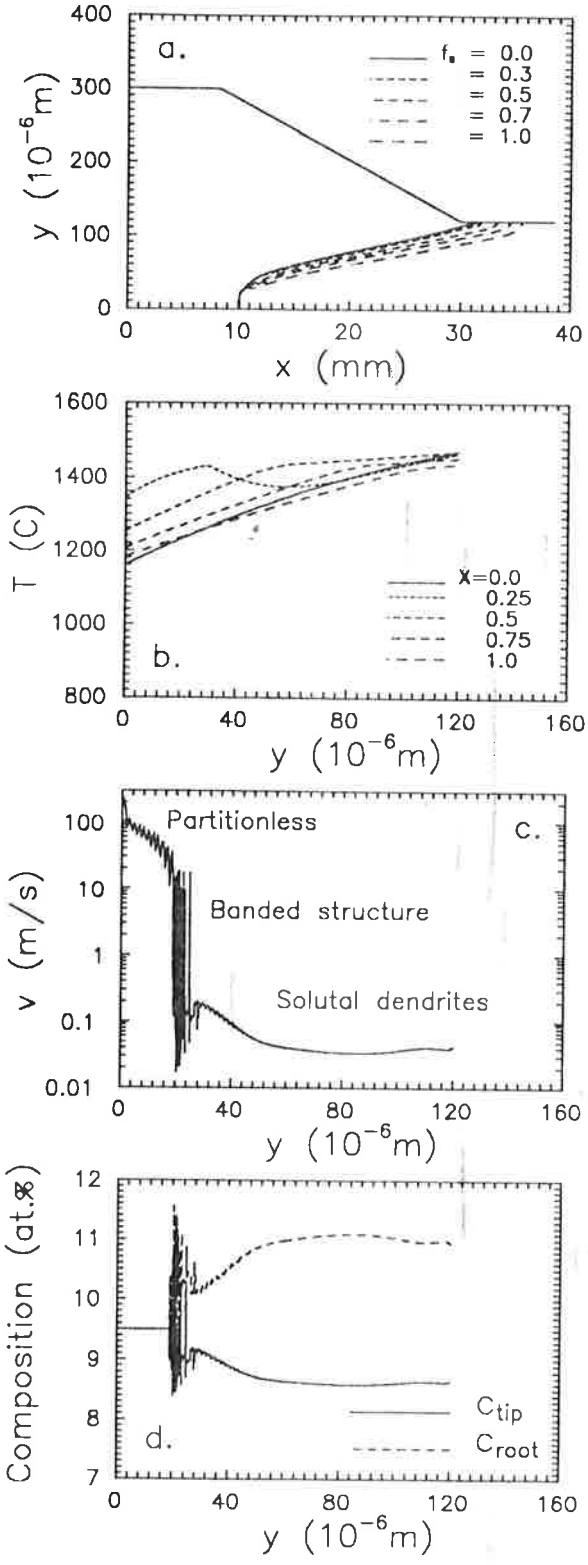

Figure 5

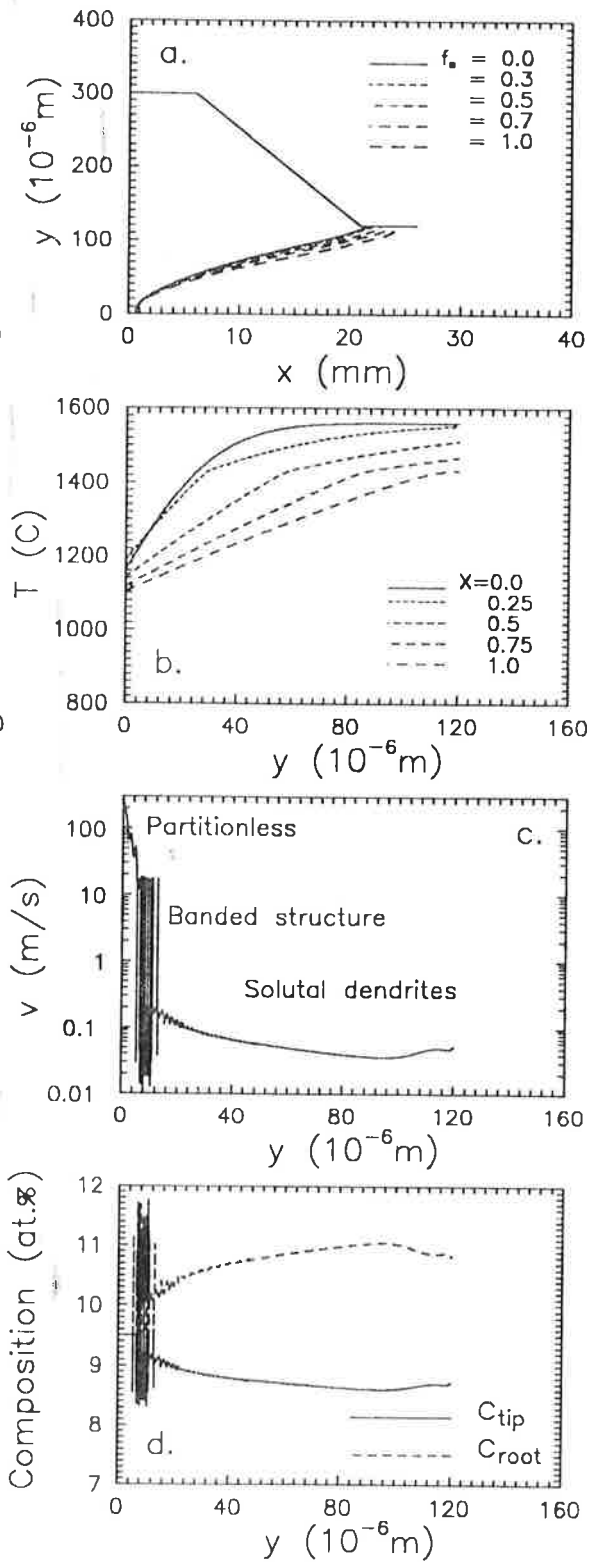

Figure 6

The effect of heat transfer coefficient on the microstructure:
Heat transfer coefficient: Figure 5 - 0.35 $MWm^{-2}K^{-1}$,
Figure 6 - 1.40 $MWm^{-2}K^{-1}$.

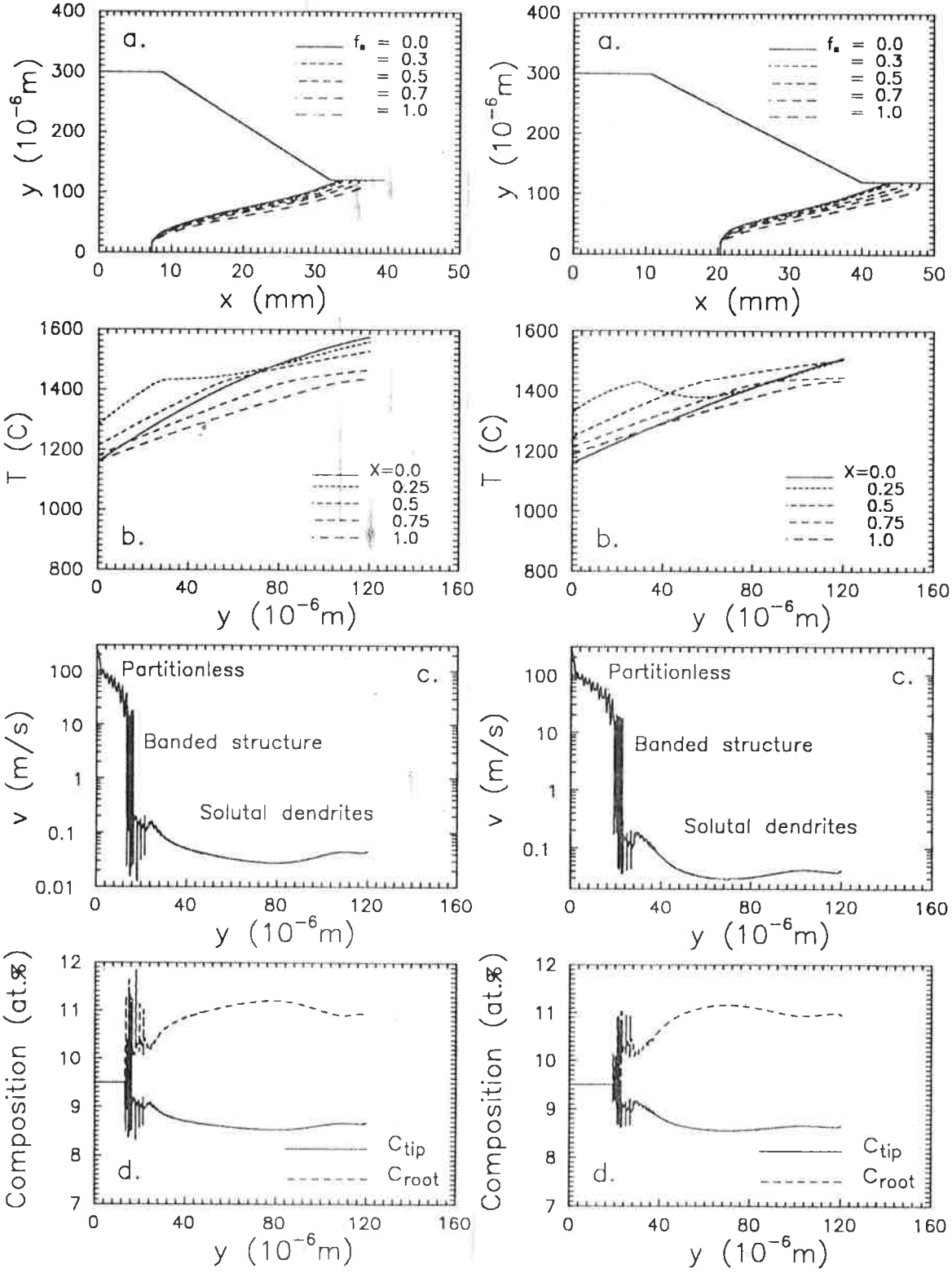

Figure 7

Figure 8

The effect of casting temperature on the microstructure:
Overheating: Figure 7 - 200 K,
Figure 8 - 300 K.

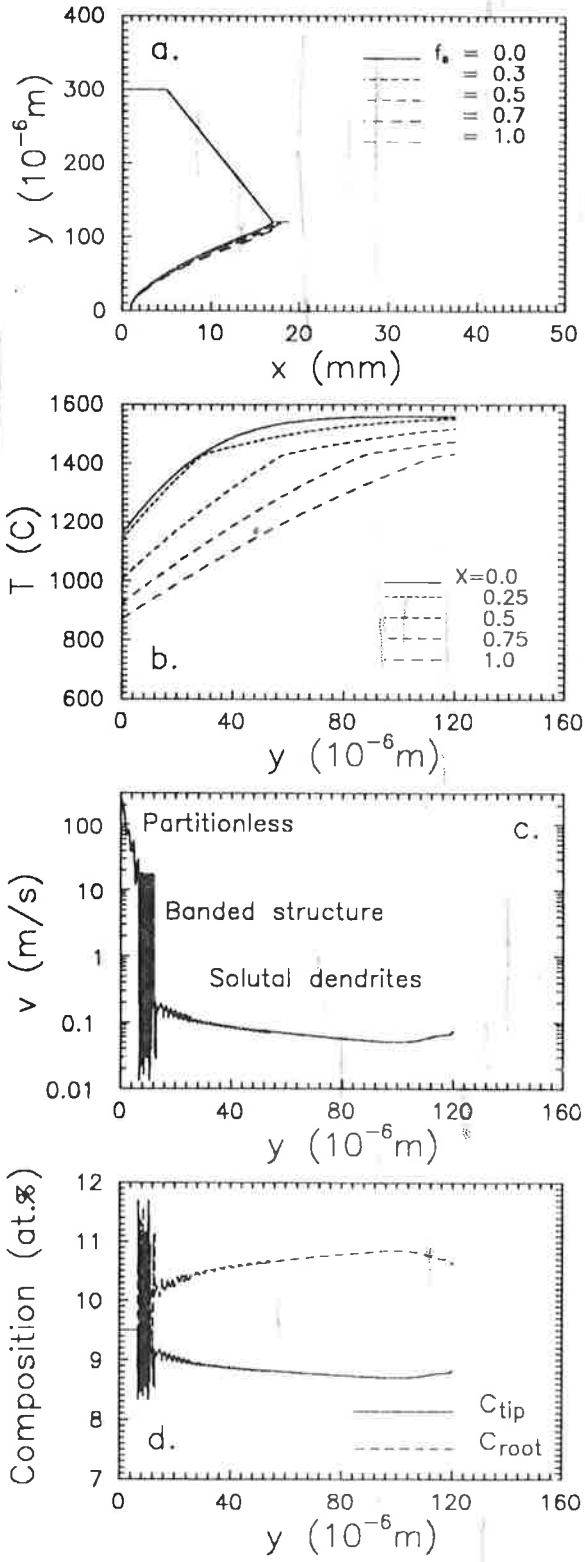

Figure 9

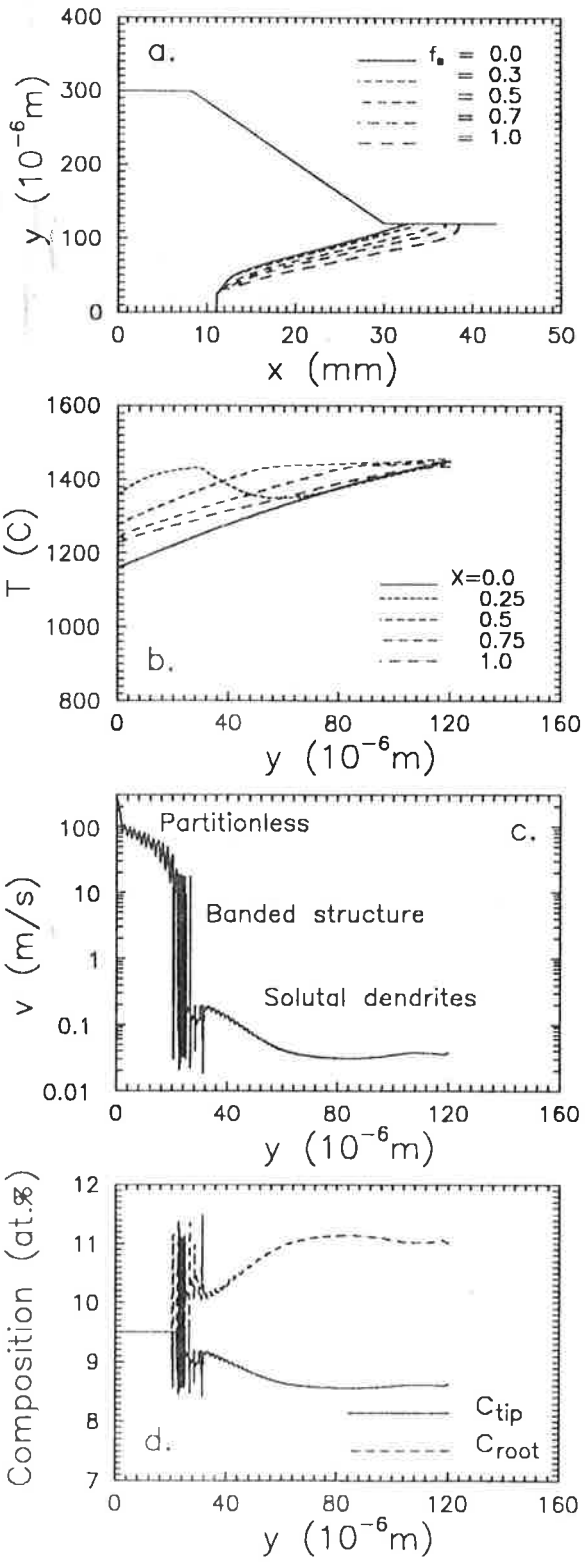

Figure 10

The effect of the materiai of roller on the microstructure:
Material of roller: Figure 9 - copper,
Figure 10 - stainless steel.

The predicted microstructure is in a global agreement with the experimental findings (5-10,31): The chill zone - identified here as the partitionless region grown with a planar morphology - can extend to the whole cross-section of thin ribbons, while a transition from chill zone to dendritic microstructure is predicted in case of thick ribbons. A remarkable discrepancy is that - although banded structures are reported for laser and electron-beam remelting, splat cooling and melt-spinning of various Al based alloys - the predicted banded structure has not been observed on Fe-Si alloys so far. It has to be mentioned, however, that the resolution of the conventional SEM is not enough to detect the composition oscillations on the predicted 100 nm scale. Systematic investigations by Auger spectroscopy, RBS, SIMS or STEM could be decisive in this case.

Effect of casting conditions on the grain size

The relation between the average grain size d and the main technological parameters has been studied on Al_2Cu, in which case both nucleation and growth are diffusion controlled. The results are summarized in Figure 11a-d. The rate of nucleation can be changed by the contact angle θ between the solid-liquid and the melt-roller interfaces. θ has been varied between 20 -70°. Since experimental data are not available for this quantity it has been used to set the grain size to a physically reasonable value. In the following computations $\theta = 50^{\circ}$ has been chosen.

Varying the casting conditions it has been found that the average grain size can be reduced by increasing the heat transfer coefficient or decreasing the roller temperature and the ribbon thickness. The grain size - heat transfer coefficient and grain size - ribbon thickness relations can be well approximated by $d \sim h^{-p}$ and $d \sim \delta^{q}$, where $p \cong 1.27$ and $q \cong 0.83$. Despite the simplified heat transport model the value obtained for q accords well with the experimental data reported for various alloys q = 0.78-1.02 (5,36). An apparent contradiction with the experiments is that according to our calculations the grain size is practically independent of the casting temperature, while a drastic reduction has been reported for increasing overheating (36). In a previous work (35) we found, however, that the heat transfer coefficient increases with overheating. Taking this effect into account the experimental trend can be reproduced.

Conclusions

The effect of casting conditions on the growth morphology and grain size has been studied by numerical methods.

A three-layer microstructure has been found for $Fe_{90.5}Si_{9.5}$, consisting a partitionless layer at the contact surface, a banded structure of partitionless and dendritic regions and a solutal dendritic region extending to the free surface. The thickness of the partitionless layer increases with increasing undercooling at nucleation, casting temperature, roller temperature and with decreasing heat transfer coefficient and heat conductivity of roller. The variation of microstructure as a function of the distance from the contact surface is independent of the ribbon thickness.

The grain size increases with increasing ribbon thickness, roller temperature and decreasing heat transfer coefficient. The predictions are in a fair agreement with the experimental results.

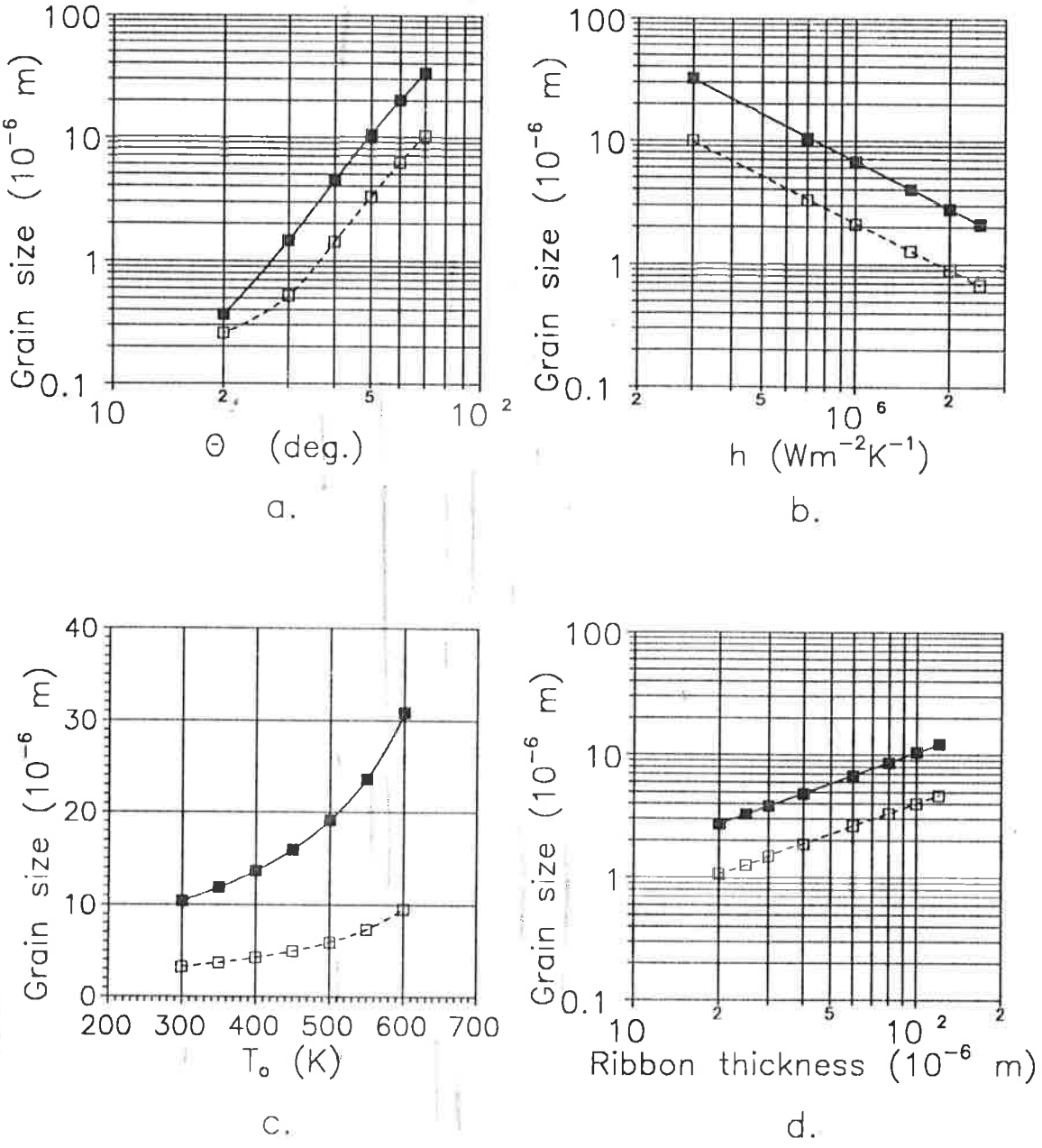

Figure 11 - The effect of casting conditions on the average grain size:
a. Grain size vs. contact angle,
b. Grain size vs. heat transfer coefficient,
c. Grain size vs. roller temperature,
d. Grain size vs. ribbon thickness.
(Notations: a-c: solid line - δ = 100 μm; dashed line - δ = 25 μm; d: solid line - h = 0.7 $MWm^{-2}K^{-1}$; dashed line - h = 1.5 $MWm^{-2}K^{-1}$.)

Acknowledgements

The authors are grateful to Dr. M.Tegze for the valuable discussions and for his help in setting up eqn. (5). One of the authors (LG) is indebted to Dr. Gy.Faigel for the computation facilities.

This work has been supported by the Hungarian Academy of Sciences under Contract OTKA-2933 and by the Deutsche Forschungsgemeinschaft under Contract No. Fr. 543/7.

References

1. "Proc. 7th Int. Conf. on Rapidly Quenched Metals", published in Mater. Sci. Eng., A133 (1991)

2. A.L.Greer, Mater. Sci. Eng., A133 (1991) 16-21

3. W.Kurz and R.Trivedi, Acta Metall. Mater., 38 (1990) 1-17

4. H.Jones, Mater. Sci. Eng., A133 (1991) 33-39

5. E.Vogt and G.Frommeyer, Z.Metallkde, 78 (1987) 262-267

6. E.Vogt, Int. J. of Rapid Solidif., 3 (1987) 131-146

8. J.Branzovsky et al., Mater. Sci. Eng., 98 (1988) 75-78

9. C.Caesar et al., ibid., 98 (1988) 339-342

10. B.Cantor et al., J. Mater. Sci., 26 (1991) 1266-1276

11. A.Ludwig, Acta Met. Mater., 39 (1991) 2795-2798

12. B.Jönsson, Mater. Sci. Eng., A133 (1991) 827-831

13. B.Jönsson, Metall. Trans., 22A (1991) 2475-2485

14. L.Gránásy and Gy.Mészáros, Mater. Sci. Eng., 72 (1985) 71-83

15. W.Kurz, B.Giovanola and R.Trivedi, Acta Metall., 34 (1986) 823-830

16. M.J.Aziz, J. Appl. Phys., 53 (1982) 1158-1168

17. J.C.Baker and J.W.Cahn, "Solidification", ASM Metals Park, OH (1971) 23

18. M.Zimmermann, M.Carrard and W.Kurz, Acta Metall., 37 (1989) 3305-3313

19. T.W.Clyne, Metal Sci., 16 (1982) 441-450

20. B.Giovanola and W.Kurz, Metall. Trans., 21A (1990) 260-263

21. T.W.Clyne, ibid., 15B (1984) 369-381

22. K.Takeshita and P.H.Shingu, Trans. JIM, 27 (1986) 454-462

23. J.W.Christian, "The Theory of Transformation in Metals and Alloys", Pergamon Press, Oxford, 1st edn., 1965

24. W.Kurz and D.J.Fischer, "Fundamentals of Solidification", Trans Tech Publ., Switzerland, 1984

25. R.Hultgren et al., "Selected Values of Thermodynamic Properties of Metals and Alloys", John Wiley & Sons, Inc., 1963

26. M.Gündüz and J.D.Hunt, Acta Metall., 33 (1985) 1651-1672

27. D.Turnbull, J. Chem. Phys., 18 (1950) 768-769

28. P.V.Evans and A.L.Greer, Mater. Sci. Eng., 98 (1988) 357-361

29. A.Ludwig, G.Frommeyer and L.Gránásy, Steel Res., 61 (1990) 467-471

30. A.Ludwig, G.Frommeyer and L.Gránásy, Mater. Sci. Eng., A133 (1991) 722-725

31. C.Taravel and D.Camel, ibid., A133 (1991) 811-818

32. G.-X.Wang and E.F.Matthys, Int. J. Rapid Solidif., 6 (1991) 141-174

33. G.-X.Wang and E.F.Matthys, Int. J. Rapid Solidif., 6 (1991) 297-324

34. L.Gránásy and A.Ludwig, Mater. Sci. Forum, 77 (1991) 211-218

35. L.Gránásy and A.Ludwig, Mater. Sci. Eng., A133 (1991) 751-754

36. E.Vogt et al., Mater. Sci. Eng., 98 (1988) 295-299